Journal of Cellular Biochemistry 101:1011–1022 (2007)

ARTICLES

Mechanisms for the Magnolol-Induced Cell Death of CGTH W-2 Thyroid Carcinoma Cells

Shih-Horng Huang,[1] Ying Chen,[2] Po-Yuan Tung,[2] Jiahn-Chun Wu,[2] Kuo-Hsin Chen,[1] Jiann-Ming Wu,[1] and Seu-Mei Wang[2]*

[1]Department of Surgery and Division of General Surgery, Far Eastern Memorial Hospital, Taipei, Taiwan 220
[2]Department of Anatomy and Cell Biology, College of Medicine, National Taiwan University, Taipei, Taiwan 10051

Abstract Magnolol, a substance purified from the bark of *Magnolia officialis,* inhibits cell proliferation and induces apoptosis in a variety of cancer cells. The aim of this study was to study the effects of magnolol on CGTH W-2 thyroid carcinoma cells. After 24 h treatment with 80 μM magnolol in serum-containing medium, about 50% of the cells exhibited apoptotic features and 20% necrotic features. Cytochrome-*c* staining was diffused in the cytoplasm of the apoptotic cells, but restricted to the mitochondria in control cells. Western blot analyses showed an increase in levels of activated caspases (caspase-3 and -7) and of cleaved poly (ADP-ribose) polymerase (PARP) by magnolol. Concomitantly, immunostaining for apoptosis inducing factor (AIF) showed a time-dependent translocation from the mitochondria to the nucleus. Inhibition of either PARP or caspase activity blocked magnolol-induced apoptosis, supporting the involvement of the caspases and PARP. In addition, magnolol activated phosphatase and tensin homolog deleted on chromosome 10 (PTEN) and inactivated Akt by decreasing levels of phosphorylated PTEN and phosphorylated Akt. These data suggest that magnolol promoted apoptosis probably by alleviating the inhibitory effect of Akt on caspase 9. Furthermore, inhibition of PARP activity, but not of caspase activity, completely prevented magnolol-induced necrosis, suggesting the notion that it might be caused by depletion of intracellular ATP levels due to PARP activation. These results show that magnolol initiates apoptosis via the cytochrome-*c*/caspase 3/PARP/AIF and PTEN/Akt/caspase 9/PARP pathways and necrosis via PARP activation J. Cell. Biochem. 101: 1011–1022, 2007.

Key words: magnolol; thyroid carcinoma cells; apoptosis; necrosis; signaling mechanism

INTRODUCTION

Studies on several cell human cancer lines have shown the potential of compounds purified from traditional Chinese herbs as anticancer drugs. One of the candidates, magnolol, isolated from the root and bark of *Magnolis officialis*, is well-known for its anti-oxidative, anti-atherosclerosis, and lipolysis and steroidogenesis-stimulating effects [Teng et al., 1988; Wang et al., 2000; Huang et al., 2004; Chen et al., 2005a,b]. Recently, attention has been paid to its anticancer action. Generally, lower concentrations of magnolol (3–40 μM) inhibit cell proliferation and high concentrations (80–100 μM) induce apoptosis of several cell lines derived from human cancers, including colon cancer, HepG2 hepatoma, leukemia cells, fibrosarcoma, melanoma, and squamous carcinoma [Lin et al., 2001, 2002; Ikeda and Nagase, 2002;

Abbreviations used: 3AB, 3, aminobenzamide; Ac-LEHD-CHO, N-acetyl-Leu-Glu-His-Asp-CHO; AIF, apoptosis inducing factor; DAPI, 4′, 6-diamidino-2-phenylindole dilactate; MTT, 3[4,5-dimethylthiazol-2-yl]-2, 5-diphenyl-tetrazolium bromide; PARP, poly (ADP-ribose) polymerase; PBS, phosphate-buffered saline; PI, propidium iodide; PI3K, phosphatidylinositol 3-kinase; PTEN, phosphatase and tensin homolog deleted on chromosome ten; Z-IETD-FMK, Z-I-E(Ome)-T-D(OMe)- fluoromethylketone; z-VAD-FMK, z-Val-Ala-Asp(OMe)-fluoromethylketone; Ac-LEHD-CHO, N-acetyl-Leu-Glu-His-Asp-CHO.

Grant sponsor: Far Eastern Memorial Hospital, Taiwan; Grant sponsor: National Science Council (NSC), Republic of China; Grant number: 94-2320-B-002-052.

*Correspondence to: Seu-Mei Wang, Department of Anatomy and Cell Biology, College of Medicine, National Taiwan University, 1-1 Jen-Ai Road, Taipei, Taiwan 10051. E-mail: smwang@ha.mc.ntu.edu.tw

Received 10 March 2006; Accepted 11 June 2006

DOI 10.1002/jcb.21100

Yang et al., 2003; Zhong et al., 2003]. In animals inoculated subcutaneously with B16-BL6 melanoma cells, magnolol effectively inhibits invasion and metastasis [Nagase et al., 2001; Ikeda and Nagase, 2002].

Several mechanisms for the magnolol-induced apoptosis of cancer cells have been proposed. These include a reduction in the mitochondrial membrane potential, cytochrome-*c* release, activation of caspases 9, 8, and 3, downregulation of Bcl-2, and upregulation of Bad and Bcl-x [Lin et al., 2001; Ikeda and Nagase, 2002; Chen et al., 2003; Yang et al., 2003; Zhong et al., 2003]. Pan-caspase or selective caspase inhibitors or overexpression of Bcl prevent magnolol-induced apoptosis of human leukemia cells and human squamous carcinoma cells [Yang et al., 2003; Zhong et al., 2003].

Other mechanisms governing apoptosis include the PI3K/Akt pathway. PTEN reduces the levels of PIP3, a second messenger generated from PI3K required for Akt phosphorylation, which then decreases Akt activity [Ali et al., 1999; Cantley and Neel, 1999]. Activation of the Akt signaling pathway appears to be an important event in thyroid tumorigenesis and tumor progression [Kada et al., 2004]. Inactivating mutation, or loss, of the *PTEN* gene is seen in human tumors of breast, prostate, thyroid, and endometrial origin. Loss or reduction of the *PTEN* gene results in hyper-activation of the PI3K/Akt signaling pathway in human malignancies [Ali et al., 1999; Cantley and Neel, 1999]. Activation of PI3K/Akt is associated with all types of thyroid carcinomas [Fagin, 2002]. Moreover, mutation of PI3KCA, the catalytic subunit of PI3K, is frequently found in anaplastic thyroid carcinoma, resulting in Akt activation [Garcia-Rostan et al., 2005]. Since the kinase activity of Akt regulates the phosphorylation of several downstream effectors, such as NF-kappa B, Bad, and GSK-3 [Mitsiades et al., 2004], inactivation of Akt by dephosphorylation can activate Bad and caspase 9, thus facilitating apoptosis [Cardone et al., 1998; Datta et al., 1999]. Importantly, the PI3K/Akt pathway controls thyroid cell proliferation by regulating the phosphorylation of p27 (kip1), an inhibitor of Cip/Kip cdk, at an ectopic position, threonine157 or 198, instead of at the normal phosphorylation sites, serine 10 and threonine 187, thus resulting in cytoplasmic sequestration of p27 in human thyroid carcinoma cells [Motti et al., 2005]. Although the importance of the cytochrome-*c*/caspase pathway has been examined [Lin et al., 2001; Ikeda and Nagase, 2002], little is known about the contribution of the PTEN/Akt pathway to the magnolol-induced apoptosis of cancer cells.

PARP is a chromatin-associated protein, and its main functions are to stabilize DNA structure and repair damaged DNA [Ha and Snyder, 1999]. Activation of caspase 3 cleaves PARP, which is then unable to repair DNA and consequently, the apoptotic process is accelerated [Ha and Snyder, 1999]. Moreover, PARP activation triggers translocation of AIF from the mitochondria to the nucleus, which also contributes to apoptosis [Susin et al., 1999]. In addition, excess PARP activation causes intracellular ATP depletion and results in necrosis [Proskuryakov et al., 2003]. Whether magnolol induces necrosis of thyroid carcinoma cells and whether PARP activation is involved remains to be examined.

In this study, we investigated the effect of magnolol on a Chinese thyroid carcinoma cell line, CGTH -W2. We identified the cell death patterns and examined whether Akt, the cytochrome-*c*/caspase pathway, and PARP activity were essential for magnolol-induced apoptosis and necrosis.

MATERIALS AND METHODS

Cell Culture

The CGTH W-2 cell line, derived from a metastatic thyroid follicular carcinoma from a Chinese patient in Taiwan, was a generous gift from Dr. Jen-Der Lin [Lin et al., 1996]. The cells were grown in RPMI 1640 containing 10% fetal bovine serum, 1 μM sodium pyruvate, and 100 IU/ml of penicillin and streptomycin, pH 7.2 (all from Gibco BRL, Grand Island, NY) in a humidified atmosphere of 5% CO_2–95% air at 37°C.

Drugs Used

Magnolol, isolated from *Magnolia officinalis* with a purity of over 99%, was purchased from the Pharmaceutical Industry Technology and Development Center, Taiwan. The PARP inhibitor, 3-aminobenzamide (3AB), was obtained from Sigma (St. Louis, MO). The general caspase inhibitor, z-Val-Ala-Asp(OMe) -fluoromethylketone (z-VAD-FMK) and the specific caspase-9 inhibitor, N-acetyl-Leu-Glu-His-Asp-CHO (Ac-LEHD-CHO), were purchased from

Biomol (Plymouth Meeting, PA). The specific caspase-8 inhibitor, Z-I-E(OMe)-T-D(OMe)-FMK (Z-IETD-FMK), was obtained from R&D sytems, Inc. (Minneapolis, MN).

MTT Test

Thyroid carcinoma cells were plated at a density of 2×10^4 cells per well in a 24-well plate and incubated for 24 h with different concentrations of magnolol in the presence or absence of 10% fetal calf serum. After two washes with phosphate-buffered saline (PBS; 137 mM NaCl, 2.7 mM KCl, 1.5 mM KH_2PO_4, 8 mM Na_2HPO_4, pH 7.3), 500 μl of RPMI medium containing 0.5 mg/ml of 3-[4,5-dimethylthiazol-2-yl]-2, 5-diphenyltetrazolium bromide (MTT; Sigma) was added to each well, then incubation was continued for 4 h to allow the conversion of the substrate into the purple formazan product. The medium was then removed and the cell lysed with 500 μl of DMSO and the absorbance at 590 nm measured with a spectrophotometer (Beckman Coulter, Inc., Fullerton, CA).

Propidium Iodide Staining for Necrotic Cells

Propidium iodide (PI; Sigma) was used to detect plasma membrane disruption in necrotic cells. Cells were treated with DMSO (vehicle control) or 80 μM magnolol for 6, 18, or 24 h; then, after washes with serum-free medium, were incubated for 30 min with PI (50 μg/ml in serum-free medium) in a CO_2 incubator. After a brief wash with PBS, the cells were fixed for 5 min in 10% formalin, washed with PBS, and mounted in fluorescence mounting medium. All experiments were performed with triplicate dishes and more than 100 cells were examined for each dish.

Assay for Apoptotic Cells

Cells were treated with DMSO (vehicle control) or magnolol for 6, 18, or 24 h, washed with PBS, and fixed for 5 min in 5% formalin and 0.5% Triton X-100 at room temperature. After a brief wash with PBS, the cells were stained for 15 min with 1 μg/ml of 4′,6-diamidino-2-phenylindole dilactate (DAPI; Sigma) in 0.9% NaCl and mounted in fluorescence mounting medium. Apoptotic cells were identified by the presence of chromatin condensation or apoptotic body formation. TUNEL staining was also performed using a kit according to the manufacture's instruction (Calbiochem, La Jolla, CA). The cells were fixed in 10% formalin in PBS, rinsed with PBS, permealized briefly, and incubated with TUNEL reaction mixture. All experiments were performed with triplicate dishes and more than 100 cells were examined per dish.

Immunocytochemistry

After treatment, cells were washed with PBS, fixed for 5 min in 10% formalin in PBS, and permeabilized for 10 min with 0.15% Triton X-100 in PBS. After PBS washes (3×5 min), non-specific binding sites were blocked by 30 min incubation at room temperature with 5% non-fat milk in PBS. The cells were then incubated overnight at 4°C with monoclonal mouse anti-cytochrome-*c* antibodies (Promega, Madison, WI) or polyclonal rabbit anti-AIF antibodies (Cell Signaling, Beverly, MA), washed with PBS, and incubated for 1 h at 37°C with fluorescein isothiocyanate-conjugated secondary antibodies (Sigma) or biotinylated goat anti-rabbit IgG and avidin-biotin-peroxidase mixture (Vector Labs, Burlingame, CA). The peroxidase reaction was then visualized by developing with the SG substrate solution (Vector Labs). For double labeling for apoptotic cells and cytochrome-*c*, cells were first immunostained for cytochrome-*c* and then stained with DAPI. Finally, the cells were washed with PBS, mounted using 3% n-propyl gallate and 50% glycerol in PBS, and examined using a Zeiss epifluorescence microscope (Carl Zeiss, Oberkocheu, Germany) equipped with a Nikon DIX digital camera (Nikon, Tokyo, Japan).

Cell Fractionation and Western Blotting

To prepare whole cell lysates, after treatment, CGTH W-2 thyroid carcinoma cells were washed once with PBS and homogenized in lysis buffer (10 mM EGTA, 2 mM $MgCl_2$, 60 mM PIPES, 25 mM HEPES, 0.15% Triton X-100, 1 μg/ml of pepstatin A, 1 μg/ml of leupeptin, 1 mM NaF, and 1 mM phenylmethylsulfonyl fluoride). To prepare the cytosolic fraction, after treatment with magnolol, CGTH W-2 thyroid carcinoma cells were briefly washed with PBS, ultrasonicated for 2×10 s in RIPA buffer (50 mM Tris-HCl, 1% Triton X-100, 0.25% Na deoxycholate, 150 mM NaCl, 1 mM EDTA, 1 mM PMSF, 1 mM NaF, 1 mM Na_3VO_4, 1 μg/ml each of aprotinin, leupeptin, and pepstatin, pH 7.4), centrifuged at 14,000*g* for 30 min at 4°C, and the supernatant taken as the cytoplasmic fraction.

For electrophoresis, an equal volume of sample buffer was added and the mixture heated at 90°C for 3 min. Proteins (40 μg per lane) were electrophoresed on a 10% SDS polyacrylamide gel and transferred to a nitrocellulose membrane (Schleicher & Schuell, Inc., Keene, NH). Strips from the membrane were then blocked by incubation for 30 min at room temperature with 5% non-fat milk in Tris-buffered saline, pH 8.2, containing 0.1% Tween (TBS-Tween) and incubated overnight at 4°C with a 1:1, dilution of monoclonal mouse antibodies against cytochrome-*c* (Promega) or rabbit antibodies against active caspase 3 (Cell Signaling), active caspase 7 (Cell Signaling), cleaved PARP (BioVision Research Products, Mountain View, CA), Akt1(Santa Cruz Biotechnology, Santa Cruz, CA), phosphorylated Akt (Santa Cruz Biotechnology), PTEN (Santa Cruz Biotechnology), or phosphorylated PTEN (Cell Signaling) diluted in TBS-Tween. After washes with TBS-Tween, the strips were incubated for 2 h at room temperature with a 1:7,500 dilution of alkaline phosphatase-conjugated anti-mouse or anti-rabbit IgG antibodies (Promega), and bound antibody was visualized using nitro blue tetrazolium and 5-bromo-4-chloro-3-indolyl phosphate (Sigma) as chromogen. The density of the bands on the nitrocellulose membrane was quantified by densitometry using Gel Pro 3.1 (Media Cybernetics, Silver Spring, MD), taking the density of the band in the control sample as 100% and expressing the density of the band in the test sample as a percentage of this. All experiments were performed at least three times, and the values are expressed as the mean ± SE.

Flow Cytometry

Isolated populations of nuclei were incubated in propidium iodide stain solution (PBS containing 0.5% Triton X-100, 50 μg/ml PI, 2 μg/ml RNAse) for 30 min at 4°C. Following incubation, nuclei were collected by centrifugation at 1,*g* for 5 min at 4°C and resuspended in 500 μl cold PBS. The samples were analyzed on a Becton-Dickinson FACS-scan (Mountain View, CA) using an argon laser (excitation 530 nm). PI fluorescence was detected using 620 nm band pass filter. Data analysis was performed using Win MDI 2.8 software program.

Statistical Analysis

All results are expressed as the mean ± SE. Statistical differences between means were assessed using Student's *t*-test, with a *P* value less than 0.05 being considered significant.

RESULTS

Magnolol Induces Apoptosis and Necrosis of CGTH W-2 Cells

In the DMSO-treated control group, CGTH W-2 cells were flattened and polygonal. The concentration of magnolol inducing cell death was dependent on the absence or presence of the serum. In the presence of serum, 24 h treatment with 40 or 60 μM magnolol decreased cell survival by 30 or 70%, respectively (Fig. 1A), whereas, in the absence of serum, only 15 or

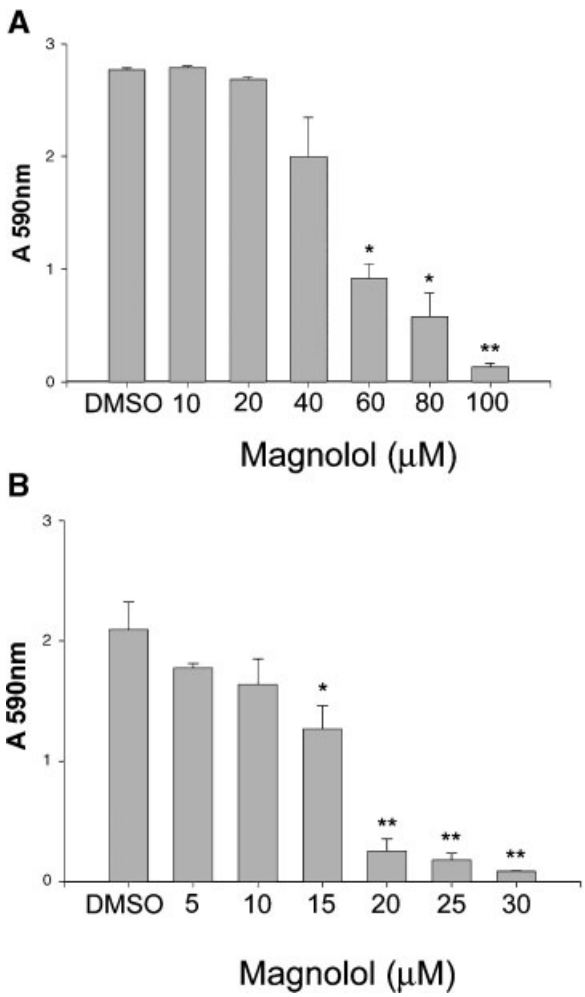

Fig. 1. Effect of magnolol on cell viability. CGTH W-2 cells were treated for 24 h with 0.1% DMSO or magnolol at various concentrations in serum-containing medium (**A**) or serum-free medium (**B**) before being processed for the MTT test. n = 3, *, $P < 0.05$; **, $P < 0.01$, compared to the DMSO group.

20 μM magnolol was required to decrease survival by 30 or 90% (Fig. 1B). Since CGTH W-2 cells became retracted after 6–24 h incubation in serum-free medium, to prevent cell distortion we performed all experiments in the serum media. In the following studies, the conditions of serum-containing medium and 80 μM magnolol were used, unless otherwise indicated. First, we identified the cell death patterns seen after 6 or 24 h treatment with 80 μM magnolol. Figure 2 shows characteristic apoptotic cells identified by DAPI staining (Fig. 2A(b); control 2A(a)) and by TUNEL staining (Fig. 2A(d); control 2A(c)). The percentages of apoptotic cells in DMSO groups are 8, 5, 5, and 3% in Figure 2B(a–d), respectively. The apoptotic ratios in plain medium appeared to be about 3–4%, lower than the values for DMSO groups, indicating the minor cytotoxic effect from DMSO alone. Quantitative analyses using different assays for apoptotic and necrotic cells confirmed the increases in apoptotic (Fig. 2B(a–c)) and necrotic cells (Fig. 2B(d)) with time of magnolol treatment. Figure. 2B(c) shows that the DNA contents in the sub-G1 regions of magnolol-treated cells were significantly greater than those in control cells. The apoptotic cell percentages estimated by DAPI staining may be higher than that by TUNEL staining at 6 h of magnolol treatment, since at the very early beginning of apoptosis, cells with chromatin condensation might be TUNEL-negative.

Signaling Pathways for Magnolol-Induced Apoptosis

To examine changes in the distribution of cytochrome-*c*, we performed both immunofluorescence and Western blot analyses. DMSO-treated control cells showed a normal appearance of the nuclei, and cytochrome-*c* was localized in the mitochondria (Fig. 3A,B). After treatment for 6 h with magnolol, the mitochondria in apoptotic cells became swollen, and an increase in the cytosolic staining of cytochrome-*c* was observed (Fig. 3C,D). The amounts of cytochrome-*c* in the cytoplasm increased with time of treatment (Fig. 4A), while those in the membrane fractions appeared unchanged by Western blotting analyses (data not shown). Our result was similar to those reported by Clark et al. [2006], which showed in the rat hippocampus after traumatic brain injury, increased levels of cytosolic cytochrome-*c* was not associated with a concomitant reduction in mitochondrial cytochrome-*c*. Since cytochrome-*c* release can activate caspase 3, we examined levels of active caspase 3, as shown by the appearance of 19 kDa and 17 kDa fragments cleaved from 30 kDa inactive procaspase 3 and found that these increased significantly after 6 h treatment with magnolol, then gradually decreased with further incubation (Fig. 4B). The 89 kDa fragment, produced from 116 kDa PARP-1 by caspase 3 activity, was not seen in DMSO control cells, but became detectable and peaked at 6 h after magnolol treatment (Fig. 4B). The levels of active caspase 3 decreased at 18 and 24 h, while those of active caspase 7 started to increase at 6 h and peaked at 18 h after magnolol treatment (Fig. 4B). Thus, increased levels of active caspase 7 might be attributed to the increased PARP cleavage after 6 h of magnolol treatment. Pretreatment with inhibitors specific for caspase 9 and 8 partially reduced the levels of active caspase 3 increased by magnolol (data not shown), indicating that caspase 3 acts distal to caspase 9 and 8. The next experiment supports that both caspase 9 and 8 contribute to the regulation of PARP cleavage, since specific inhibitors of these two caspases partially or completely prevented magnolol-induced PARP cleavage (Fig. 4C).

Activation of PARP-1 triggers the release of AIF from mitochondria and translocation to the nucleus [Susin et al., 1999]. In DMSO-treated cells, AIF was restrictively localized in the mitochondria (Fig. 5A), while, after 6–24 h of treatment with magnolol, diffuse staining of AIF was noted in the nuclei, a sign of nuclear translocation (Fig. 5B–D). The percentages of AIF-positive nuclei increased with time of magnolol treatment (Fig. 5). To confirm the involvement of caspase and PARP activation in magnolol-induced apoptosis, we treated the cells with the PARP inhibitor, 3AB, the general caspase inhibitor, z-VAD-FMK, the caspase-8 inhibitor, Z-IETD-FMK or the caspase-9 inhibitor, Ac-LEHD-CHO, for 30 min before, and during, incubation for 6 h with magnolol. Treatment with different inhibitor alone did not affect the proportions of apoptotic cells. Inhibiting the activities of total caspases or caspase 9 significantly blocked the induction of apoptosis by magnolol (Fig. 6A). The specific caspase-8 inhibitor partially decreased the percentages of apoptotic cells induced by magnolol without reaching statistical significance. Inhibition of PARP activity by 3AB also largely

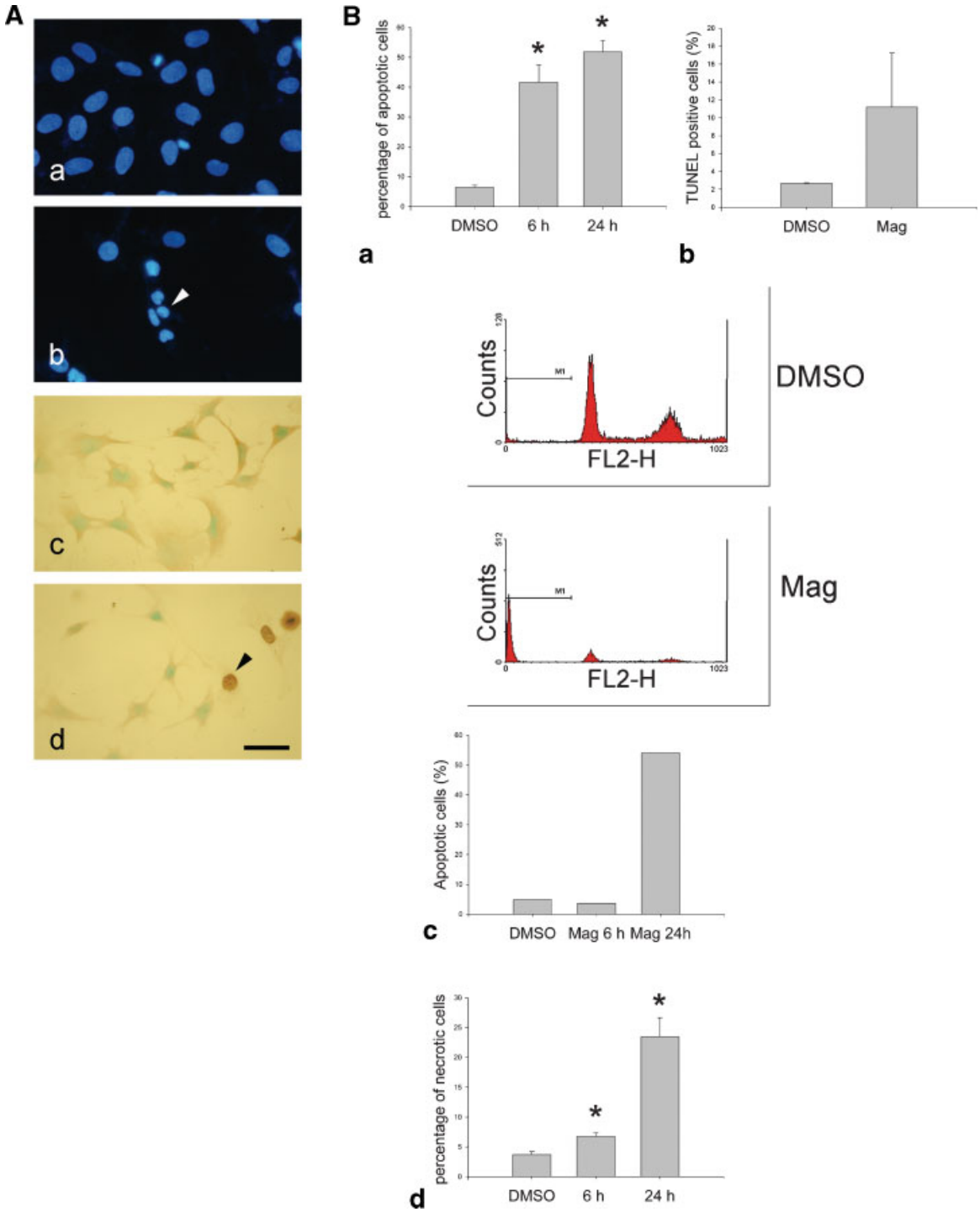

Fig. 2. Analyses of apoptotic and necrotic cells induced by magnolol. **A**: Cells were treated for 6h with 0.1% DMSO (a, c) or 80 μM magnolol (Mag) (b, d) in serum medium. Apoptotic cells were identified by nuclear condensation after DAPI staining (b; control a), or by TUNEL positivity (d; control c). Bar = 40 μm. **B**: Quantitative analyses of apoptotic and necrotic cells by magnolol. The percentages of apoptotic cells were evaluated by DAPI staining (a) or TUNEL staining (b). A representative result from flow cytometry is shown in (c). Necrotic cells were vitally stained with PI (d). n = 3. *, $P < 0.05$, compared to the DMSO group.

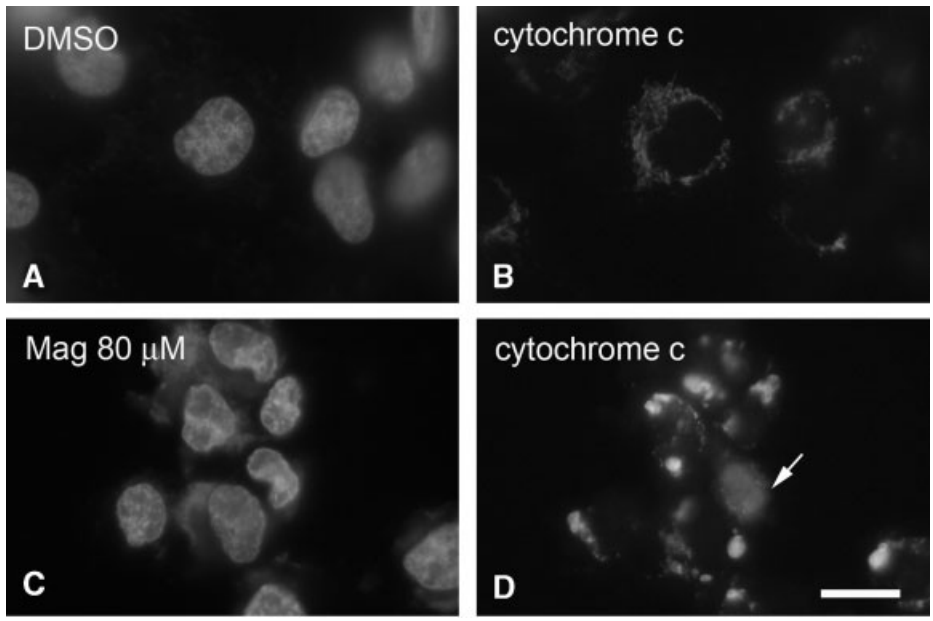

Fig. 3. Distribution of cytochrome-*c* in magnolol-treated cells. Cells were treated for 6 h with DMSO (**A**, **B**) or 80 μM magnolol (**C**, **D**), then processed for cytochrome-*c* immunostaining (B, D) or DAPI staining (A, C). The arrow indicates cytosolic staining for cytochrome-*c* in apoptotic cells. Bar = 20 μm.

prevented induction of apoptosis by magnolol (Fig. 6A). This effect may be explained by the observation that 3AB partially prevented the magnolol-induced PARP cleavage (Fig. 4C), therefore, allowing more PARP for repairing damaged DNA. In addition, the protective effect of 3AB may be due to inhibition of AIF translocation by inactivating PARP, as supported by the findings that PARP-deficiency and PARP inhibitor block AIF-induced apoptosis [Boulares et al., 1999; Yu et al., 2002; Zhang et al., 2005]. Thus, the apoptosis triggered by magnolol is both caspase- and PARP-dependent.

Levels of phosphorylated PTEN, an active form of PTEN, were decreased with time of magnolol treatment, concomitantly with a late decrease in PTEN expression after 24 h treatment (Fig. 7A). PTEN can inactivate Akt by dephosphorylating it. As expected, the levels of phosphorylated Akt (inactive Akt), were significantly decreased by magnolol, in accomplishment with its downregulation (Fig. 7B).

Mechanisms for Magnolol-Induced Necrosis

DNA damage increases PARP activity, resulting in depletion of intracellular ATP, which might result in necrosis. When PARP activity was inhibited by 3AB, induction of necrosis by magnolol was completely prevented (Fig. 6B). Inhibition of caspases had no such effect.

DISCUSSION

Previous studies demonstrated the apoptotic effect of magnolol on several human cancer cell types and that the pathway mediating apoptosis is the cytochrome-*c*/caspase 3 cascade [Lin et al., 2001; Yang et al., 2003]. The present work extended these studies to human thyroid carcinoma cells. In addition to the major apoptosis pathway, necrosis was found to be a minor contributor to magnolol-induced cell death in this cell type.

Using immunofluorescence and Western blotting analyses, we demonstrated cytochrome-*c* release in the cytoplasm of apoptotic cells. Furthermore, activations of caspase 3 and caspase 7 were observed after 6 and 18 h of magnolol treatment, respectively. The involvement of caspases was further confirmed by the observation that a pan-caspase inhibitor completely inhibited magnolol-induced apoptosis. Consistent with a previously reported mechanism for magnolol in other cell cancer cells, we showed that the cytochrome-*c*/caspase 3 pathway contributed to the magnolol-induced apoptosis of thyroid carcinoma cells. Interestingly, we found that either a pan caspase inhibitor or

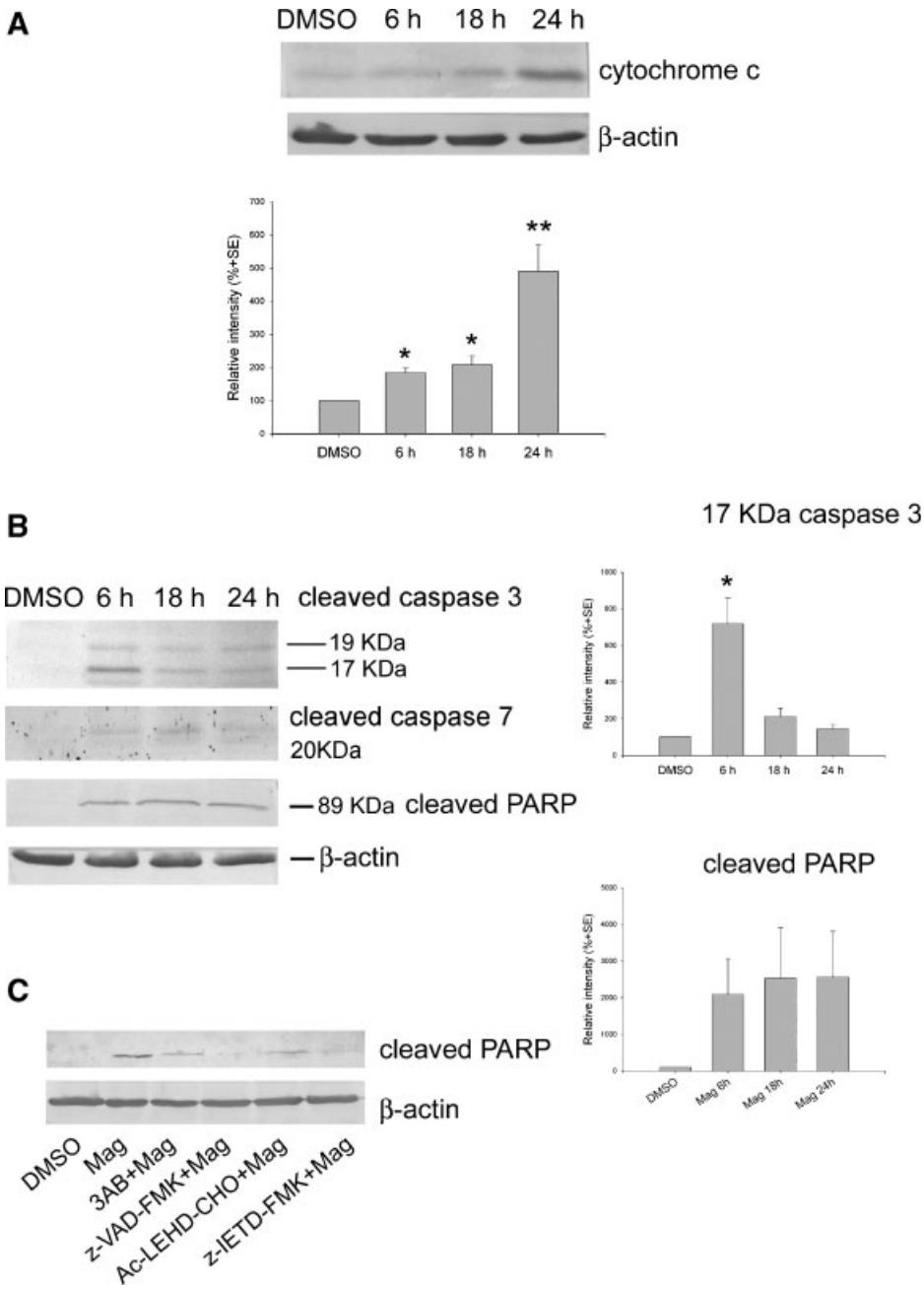

Fig. 4. Effect of magnolol on levels of cytochrome-*c*, active caspase 3, and cleaved PARP. Cells were treated with DMSO and 80 μM magnolol for 6, 18, or 24 h. Western blotting showing analysis of the cytosolic and membranous fractions for cytochrome-*c* (**A**) or of the total cell lysates for active caspase 3 (17 and 19 kDa), active caspase 7 (20 kDa), cleaved PARP (89 kDa), or β-actin (loading control). **B**: A typical blot and densitometric scans of triplicate blots are shown. *, $P < 0.05$; **, $P < 0.01$ compared to the DMSO group. **C**: Effect of different caspase inhibitors on magnolol-induced PARP cleavage. Cells were pretreated with different inhibitors (50 μM z-VAD-FMK, 1 mM 3AB, 50 μM Ac-LEHD-CHO, 50 μM Z-IETD-FMK) for 30 min before, and during, 6 h incubation with 80 μM magnolol, then cell homogenates analyzed for cleaved PARP levels.

a caspase-9 inhibitor but not the caspase-8 inhibitor caused complete block of magnolol-induced apoptosis. The data suggest that caspase 9 acts as the upstream molecule to activate caspase 3. Several intrinsic pathways account for cytochrome-*c* release from mitochondria, such as the translocation of Bax to, and competition with Bcl-2 in, the mitochondrial membrane, the translocation to the mitochondria of a truncated form of Bid formed by

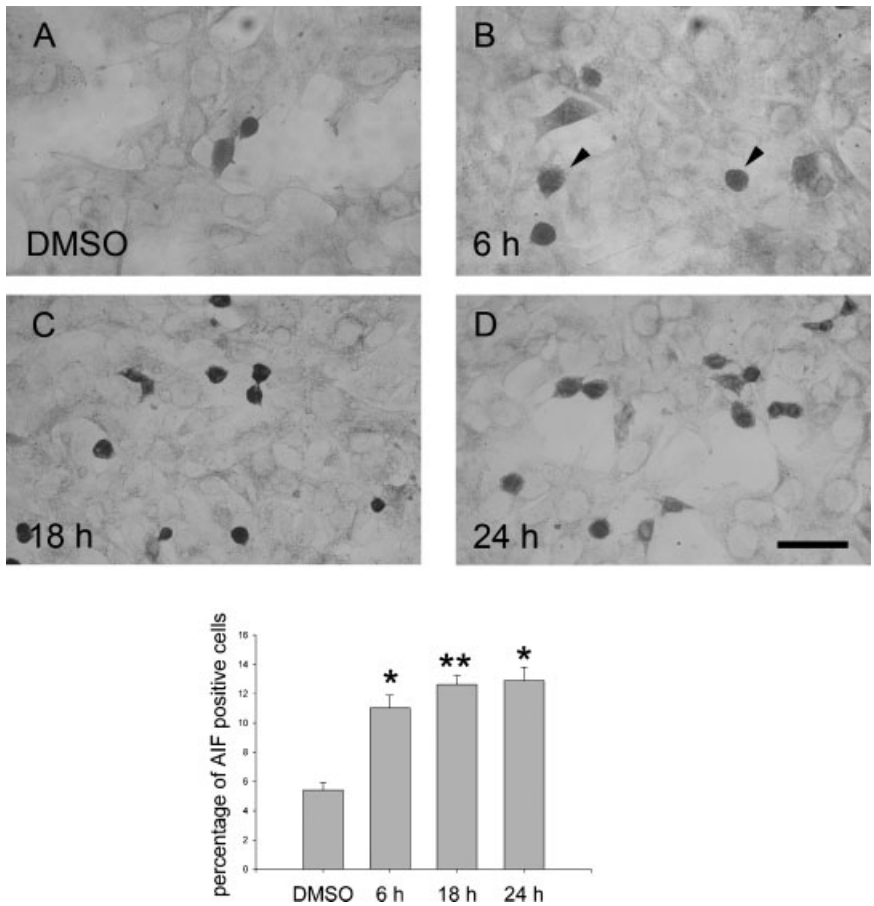

Fig. 5. Time course study of magnolol-induced translocation of AIF. Cells were treated with DMSO for 24 h (**A**) or 80 μM magnolol for 6 (**B**), 18 (**C**), or 24 h (**D**) and immunostained for AIF. The localization of AIF in magnolol-treated cells was visualized by biotin-avidin-peroxidase method. Bar = 20 μm. **Lower panel**: Time course analysis of AIF-positive cells after magnolol treatment. n = 3, *, $P < 0.05$; **, $P < 0.01$, compared to the DMSO group.

caspase 8 activity, the loss of the mitochondrial membrane potential, or the opening of permeability transition pores upon Ca^{2+} overload [Smaili et al., 2000; Ferrer and Planas, 2003]. The mechanism by which magnolol induces cytochrome-*c* release remains to be studied.

PARP is primarily activated by DNA breaks, and mild activation facilitates DNA repair and cell survival [Virag, 2005]. In early apoptosis, this enzyme activated may accelerate the apoptotic cascade by mediating the translocation of AIF from the mitochondria to the nucleus. However, excessive DNA damage induces over activation of PARP, which switches the mode of cell death from apoptosis to necrosis by consuming NAD^+ and ATP. Consistent with the above hypotheses, this study provided evidence that magnolol caused PARP activation, as shown by AIF translocation from the mitochondria to the nucleus, and PARP activation was necessary for the effect of magnolol on apoptosis and necrosis, since PARP inhibition by 3AB abrogated these effects. Nuclear translocation of AIF is known to induce peripheral chromatin condensation and large-scale DNA fragmentation [Susin et al., 1999; Yu et al., 2002, 2003]. Thus, inhibition of PARP activity by 3AB might block AIF translocation from the mitochondria to the nucleus, thus preventing DNA damage [Yu et al., 2003; van Wijk and Hageman, 2005]. PARP is cleaved at the late apoptotic phase by caspase 3 or caspase 7 [Decker and Muller, 2002]. In this study, early activation of caspase 3 and late activation of caspase 7 apparently contributed to the time-dependent increase in cleaved PARP. One of the cleaved PARP fragments, the N-terminal DNA-binding domain, promotes apoptosis by preventing DNA

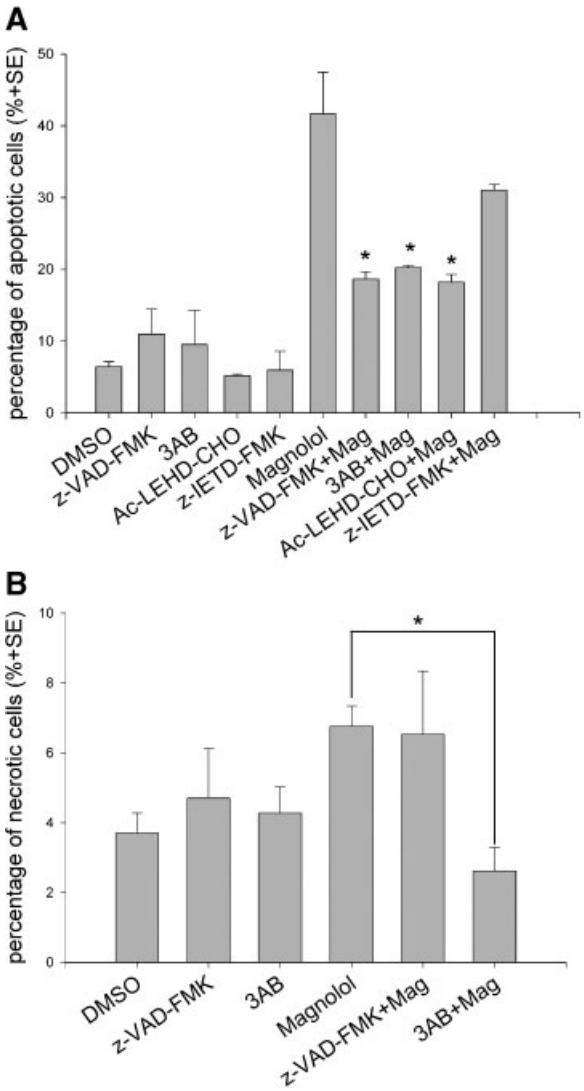

Fig. 6. Effect of a PARP inhibitor or caspase inhibitors on magnolol-induced cell death. Cells were incubated with inhibitors alone or in the presence of different inhibitors (50 μM z-VAD-FMK, 1 mM 3AB, 50 μM Ac-LEHD-CHO, or 50 μM Z-IETD-FMK) for 30 min before, and during, 6 h incubation with 80 μM magnolol, then stained with PI or DAPI to calculate the percentage of apoptotic (**A**) or necrotic cells (**B**). n = 3, *, $P < 0.05$ compared to the magnolol-treated group.

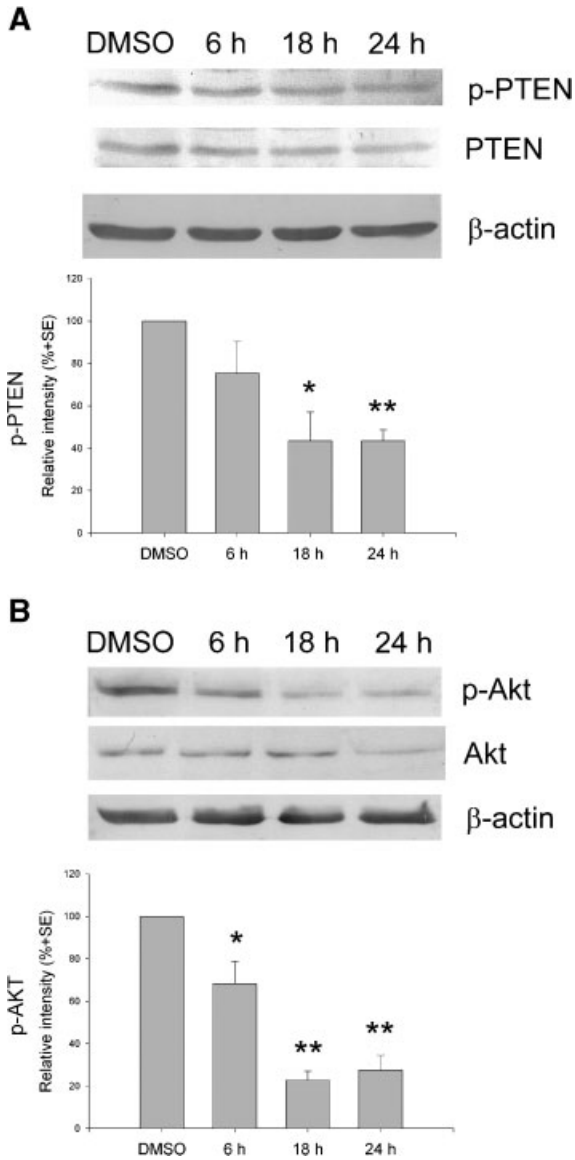

Fig. 7. Changes in the total and phosphorylation levels of PTEN and Akt after magnolol treatment. Cells were treated with DMSO or 80 μM magnolol for different intervals (6, 18, or 24 h), then the cell homogenates were analyzed for PTEN (**A**), p-PTEN (A), Akt (**B**), and p-Akt (B) by Western blotting. β-actin, loading control. A typical blot and data on densitometric scans of triplicate blots for p-PTEN (A, **lower panel**) and p-Akt (B, lower panel) were shown. *, $P < 0.05$; **, $P < 0.01$, compared to the DMSO group.

repair-induced survival, since it binds strongly to DNA and inhibits the catalytic activity of intact PARP-1 [D'Amours et al., 2001].

PTEN dephosphorylates inositol phospholipid intermediates of the PI3K pathway, thus inhibiting activation of the downstream target, Akt [Ali et al., 1999; Cantley and Neel, 1999]. In the present study, magnolol induced PTEN activation and downregulation and dephosphorylation of Akt. The reduction in phosphorylated Akt levels correlated with a decrease in PTEN phosphorylation at the same time point. Inactivation of Akt by dephosphorylation removes its inhibitory effect on several components of the cell death machinery, such as Bad and caspase 9, which, in turn, induce apoptosis [Cardone et al., 1998; Datta et al., 1999]. The reason why the caspase-9 inhibitor caused complete inhibition of magnolol-induced apoptosis may be due to the fact that caspase 9 is the

common downstream effector of both the Akt and cytochrome-*c*/caspase cascades. In addition, inactivation of Akt activates GSK3β, resulting in destabilization of cyclin D1 and upregulation of p27, thus inhibiting the cell cycle [Motti et al., 2005]. This downregulation of Akt activity provides another possible mechanism for magnolol-induced apoptosis.

Recent studies also suggest that PTEN can suppress the invasiveness and motility of various types of tumor cells [Koul et al., 2001; Raftopoulou et al., 2004]. Akt inactivation via dephosphorylation reduces the invasiveness of melanoma and bladder cancer cells [Stewart et al., 2003; Wu et al., 2004; Franke et al., 2005]. Previous studies have shown that magnolol has an inhibitory effect of invasiveness and metastasis of melanoma [Nagase et al., 2001; Ikeda and Nagase, 2002]. Our findings that magnolol induced PTEN activation and Akt inactivation may account for these effects. A study of the effect of magnolol on the invasiveness and motility of CGTH W-2 cells is currently underway. The regulation of PTEN expression is poorly understood. PPARγ agonists have been shown to upregulate PTEN expression in pancreatic cancer cells [Farrow and Evers, 2003] and non-small cell lung cancer cells [Lee et al., 2006]. In human umbilical vein endothelial cells, sphingosine-1-phosphate acts through the S1P2R receptor, a G-protein-coupled receptor, to increase PTEN activity by tyrosine phosphorylation [Sanchez et al., 2005]. Understanding how magnolol upregulates PTEN expression is of considerate interest. Thus, magnolol may represent a new therapy for the treatment of thyroid cancers.

Necrosis also contributed to the magnolol-induced cell death. PARP has been implicated in apoptosis and necrosis. PARP overactivation consumes NAD^+, and depletes intracellular energy stores, thus resulting in cell dysfunction or necrosis [Ha and Snyder, 1999; Herceg and Wang, 1999]. The involvement of PARP activation in the induction of necrosis by magnolol was confirmed by the observation that the PARP inhibitor, 3AB, successfully abolished magnolol-induced necrosis. In conclusion, we provide evidence that, in response to magnolol treatment, CGTH W-2 thyroid carcinoma cells die mainly due to apoptosis, with a minor contribution from necrosis. Apoptosis is mediated by the cytochrome-*c*/caspase 3/PARP and PTEN/Akt pathways and necrosis by the PARP pathway.

ACKNOWLEDGMENTS

We thank Dr. Thomas Barkas for his critical reading and correction of this manuscript.

REFERENCES

Ali IU, Schriml LM, Dean M. 1999. Mutational spectra of PTEN/MMAC1 gene: A tumor suppressor with lipid phosphatase activity. J Natl Cancer Inst 91:1922–1932.

Boulares AH, Yakovlev AG, Ivanova V, Stoica BA, Wang G, Iyer S, Smulson M. 1999. Role of poly(ADP-ribose) polymerase (PARP) cleavage in apoptosis. Caspase 3-resistant PARP mutant increases rates of apoptosis in transfected cells. J Biol Chem 274:22932–22940.

Cantley LC, Neel BG. 1999. New insights into tumor suppression: PTEN suppresses tumor formation by restraining the phosphoinositide 3-kinase/AKT pathway. Proc Natl Acad Sci USA 96:4240–4245.

Cardone MH, Roy N, Stennicke HR, Salvesen GS, Franke TF, Stanbridge E, Frisch S, Reed JC. 1998. Regulation of cell death protease caspase-9 by phosphorylation. Science 13:1318–1321.

Chen JS, Chen YL, Greenberg AS, Chen YJ, Wang SM. 2005a. Magnolol stimulates lipolysis in lipid-laden RAW 264.7 macrophages. Cell Biochem 94:1028–1037.

Chen YC, Chang MF, Chen Y, Wang SM. 2005b. Signaling pathways of magnolol-induced adrenal steroidogenesis. FEBS Lett 579:4337–4343.

Chen JH, Wu CC, Hsiao G, Yen MH. 2003. Magnolol induces apoptosis in vascular smooth muscle. Naunyn Schmiedebergs Arch Pharmacol 368:127–133.

Clark RS, Nathaniel PD, Zhang X, Dixon CE, Alber SM, Watkins SC, Melick JA, Kochanek PM, Graham SH. 2006. boc-Aspartyl(OMe)-fluoromethylketone attenuates mitochondrial release of cytochrome c and delays brain tissue loss after traumatic brain injury in rats. J Cereb Blood Flow Metab (Online published).

Datta SR, Brunet A, Greenberg ME. 1999. Cellular survival: A play in three Akts. Genes Dev 15:2905–2927.

D'Amours D, Sallmann FR, Dixit VM, Poirier GG. 2001. Gain-of-function of poly(ADP-ribose) polymerase-1 upon cleavage by apoptotic proteases: Implications for apoptosis. J Cell Sci 114:3771–3778.

Decker P, Muller S. 2002. Modulating poly (ADP-ribose) polymerase activity: Potential for the prevention and therapy of pathogenic situations involving DNA damage and oxidative stress. Curr Pharm Biotechnol 3:275–283.

Fagin JA. 2002. Minireview: Branded from the start-distinct oncogenic initiating events may determine tumor fate in the thyroid. Mol Endocrinol 6:903–911.

Farrow B, Evers BM. 2003. Activation of PPARgamma increases PTEN expression in pancreatic cancer cells. Biochem Biophys Res Commun 301:50–53.

Ferrer I, Planas AM. 2003. Signaling of cell death and cell survival following focal cerebral ischemia: Life and death struggle in the penumbra. J Neuropathol Exp Neurol 62: 329–339.

Franke TF, Hornik CP, Segev L, Shostak GA, Sugimoto C. 2005. PI3K/Akt and apoptosis: Size matters. Oncogene 22:8983–8998.

Garcia-Rostan G, Costa AM, Pereira-Castro I, Salvatore G, Hemandez R, Hermsem MJ, Herrero A, Fusco A, Camaselle-Teijeiro J, Santoro M. 2005. Mutation of the

PIK3CA gene in anaplastic thyroid cancer. Cancer Res 15:10199–10207.
Ha HC, Snyder SH. 1999. Poly(ADP-ribose) polymerase is a mediator of necrotic cell death by ATP depletion. Proc Natl Acad Sci USA 96:13978–13982.
Herceg Z, Wang ZQ. 1999. Failure of poly (ADP-ribose) polymerase cleavage by caspases leads to induction of necrosis and enhanced apoptosis. Mol Cell Biol 19:5124–5133.
Huang SH, Shen WJ, Yeo HL, Wang SM. 2004. Signaling pathway of magnolol-stimulated lipolysis in sterol ester-loaded 3T3-L1 preadipocytes. J Cell Biochem 91:1021–1029.
Ikeda K, Nagase H. 2002. Magnolol has the ability to induce apoptosis in tumor cells. Biol Pharm Bull 25:1546–1549.
Kada F, Saji M, Ringel MD. 2004. Akt: A potential target for thyroid cancer therapy. Curr Drug Targets Immune Endocr Metabol Disord 4:181–185.
Koul D, Parthasarathy R, Shen R, Davies MA, Jasser SA, Chintala SK, Rao JS, Sun Y, Benvenisite EN, Liu TJ, Yung WK. 2001. Suppression of matrix metalloproteinase-2 gene expression and invasion in human glioma cells by MMAC/PTEN. Oncogene 20:6669–6678.
Lee SY, Hur GY, Jung KH, Jung HC, Lee SY, Kim JH, Shin C, Shim JJ, In KH, Kang KH, Yoo SH. 2006. PPAR-gamma agonist increase gefitinib's antitumor activity through PTEN expression. Lung Cancer 51:297–301.
Lin JD, Jeng LB, Chao TC, Weng HF, Huang HS. 1996. Surgical treatment of papillary and follicular thyroid carcinoma. Int Surg 81:61–66.
Lin SY, Chang YT, Liu JD, Yu CH, Ho YS, Lee YH, Lee WS. 2001. Molecular mechanisms of apoptosis induced by magnolol in colon and liver cancer cells. Mol Carcinog 32: 73–83.
Lin SY, Lau JD, Chang HC, Yeh SD, Lin CH, Lee WS. 2002. Magnolol suppresses proliferation of cultured human colon and liver cancer cells by inhibiting DNA synthesis and activating apoptosis. J Cell Biochem 84:532–544.
Mitsiades CS, Mitsiades N, Koutsilieris M. 2004. The Akt pathway: Molecular targets for anti-cancer drug development. Curr Cancer Drug Targets 4:235–256.
Motti ML, Califano D, Troncone G, De Marco C, Migliaccio I, Palmieri E, Pezzullo L, Palombini L, Fusco A, Viglietto G. 2005. Complex regulation of the cyclin-dependent kinase inhibitor p27kip1 in thyroid cancer cells by the PI3K/AKT pathway: Regulation of p27kip1 expression and localization. Am J Pathol 166:737–749.
Nagase H, Ikeda K, Sakai Y. 2001. Inhibitory effect of magnolol and honokiol from Magnolia obovata on human fibrosarcoma HT-1080. Invasiveness in vitro. Planta Med 67:705–708.
Proskuryakov SY, Konoplyannikov AG, Gabai VL. 2003. Necrosis: A specific form of programmed cell death? Exp Cell Res 1:1–16.
Raftopoulou M, Etienne-Manneville S, Self A, Nicholls S, Hall A. 2004. Regulation of cell migration by the C2 domain of the tumor suppressor PTEN. Science 303: 1179–1181.
Sanchez T, Thangada S, Wu MT, Kontos CD, Wu D, Wu H, Hla T. 2005. PTEN as an effector in the signaling of antimigratory G protein-coupled receptor. Proc Natl Acad Sci USA 102:4312–4317.
Smaili SS, Hsu YT, Youle RJ, Russell JT. 2000. Mitochondria in Ca2+ signaling and apoptosis. J Bioenerg Biomembr 32:35–46.
Stewart J, Siavash H, Hebert C, Norris K, Nikitakis NG, Sauk JJ. 2003. Phenotypic switching of VEGF and collagen XVIII during hypoxia in head and neck squamous carcinoma cells. Oral Oncol 39:862–869.
Susin SA, Lorenzo HK, Zamzami N, Marzo I, Snow BE, Brothers GM, Mangion J, Jacotot E, Costantini P, Loeffler M, Larochette N, Goodlett DR, Aebersold R, Siderovski DP, Penninger JM, Kroemer G. 1999. Molecular characterization of mitochondrial apoptosis-inducing factor. Nature 397:441–446.
Teng CM, Chen CC, Ko FN, Lee LG, Huang TF. 1988. Two anti-platelet agents from Magnolia officinalis. Thromb Res 50:757–765.
van Wijk SJ, Hageman GJ. 2005. Poly(ADP-ribose) polymerase-1 mediated caspase-independent cell death after ischemia/reperfusion. Free Radic Biol Med 1: 81–90.
Virag L. 2005. Structure and function of poly(ADP-ribose) polymerase-1: Role in oxidative stress-related pathologies. Curr Vasc Pharmacol 3:209–214.
Wang SM, Lee LJ, Huang YT, Chen JJ, Chen YL. 2000. Magnolol stimulates steroidogenesis in rat adrenal cells. Br J Pharmacol 131:1172–1178.
Wu X, Obata T, Khan Q, Highshaw RA, De Vere White R, Sweeney C. 2004. The phosphatidylinositol-3 kinase pathway regulates bladder cancer cell invasion. BJU Int 93:143–150.
Yang SE, Hsieh MT, Tsai TH, Hsu SL. 2003. Effector mechanism of magnolol-induced apoptosis in human squamous carcinoma CH27 cells. Br J Pharmacol 138: 193–201.
Yu SW, Wang H, Poitras MF, Coombs C, Bowers WJ, Federoff HJ, Poirier GG, Dawson TM, Dawson VL. 2002. Mediation of poly(ADP-ribose) polymerase-1-dependent cell death by apoptosis-inducing factor. Science 297:259–263.
Yu SW, Wang H, Dawson TM, Dawson VL. 2003. Poly(ADP-ribose) polymerase-1 and apoptosis inducing factor in neurotoxicity. Neurobiol Dis 14:303–317.
Zhang Y, Zhang X, Park TS, Gidday JM. 2005. Cerebral endothelial cell apoptosis after ischemia-reperfusion: Role of PARP activation and AIF translocation. J Cereb Blood Flow Metab 25:868–877.
Zhong WB, Wang CY, Ho KJ, Lu FJ, Chang TC, Lee WS. 2003. Magnolol induces apoptosis in human leukemia cells via cytochrome c release and caspase activation. Anticancer drugs 14:211–217.